

## Influence of Magnetic Fields on Electron-Ion Recombination at Very Low Energies

G. Gwinner,<sup>1</sup> A. Hoffknecht,<sup>2</sup> T. Bartsch,<sup>2</sup> M. Beutelspacher,<sup>1</sup> N. Eklöv,<sup>3</sup> P. Glans,<sup>3,\*</sup> M. Grieser,<sup>1</sup>  
S. Krohn,<sup>1</sup> E. Lindroth,<sup>3</sup> A. Müller,<sup>2</sup> A. A. Saghir,<sup>1</sup> S. Schippers,<sup>2</sup> U. Schramm,<sup>1</sup> D. Schwalm,<sup>1</sup>  
M. Tokman,<sup>3</sup> G. Wissler,<sup>1</sup> and A. Wolf<sup>1</sup>

<sup>1</sup>Max-Planck-Institut für Kernphysik, 69117 Heidelberg, Germany

<sup>2</sup>Institut für Kernphysik, Universität Giessen, 35392 Giessen, Germany

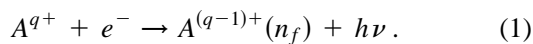
<sup>3</sup>Stockholm University, 10405 Stockholm, Sweden

(Received 12 November 1999)

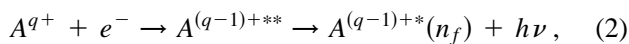
Radiative recombination (inverse photoionization) is believed to be well understood since the beginning of quantum mechanics. Still, modern experiments consistently reveal excess recombination rates at very low electron-ion center-of-mass energies. In a detailed study on recombination of  $F^{6+}$  and  $C^{6+}$  ions with magnetically guided electrons we explored the yet unexplained rate enhancement, its dependence on the magnetic field  $B$ , the electron density  $n_e$ , and the beam temperatures  $T_{\perp}$  and  $T_{\parallel}$ . The excess scales as  $T_{\perp}^{-1/2}$  and, surprisingly, as  $T_{\parallel}^{-1/2}$ , increases strongly with  $B$ , and is insensitive to  $n_e$ . This puts strong constraints on explanations of the enhancement.

PACS numbers: 34.80.Lx

Recombination between free electrons and ions is a fundamental process relevant to many areas of basic and applied physics such as atomic structure, astrophysics, fusion plasmas, accelerator physics, and the production of anti-hydrogen. Heavy-ion storage rings equipped with electron coolers have been extensively used for recombination studies in merged beams at high-energy resolution during the past decade [1]. For electron densities in present electron coolers or targets the two dominating recombination channels are radiative recombination (RR) and dielectronic recombination (DR). Radiative recombination is a nonresonant one-step process in which a free electron is captured into a bound state of an ion with simultaneous emission of a photon (reverse photoionization):



Dielectronic recombination, in contrast, is a two-step process, where resonant dielectronic capture (inverse Auger process) into a doubly excited state is followed by radiative stabilization:



where the final states  $n_f$  typically must have binding energies of  $\geq 0.3$  eV to be observed in the experiments. By using electron and ion beams of nearly matched velocities, low collision energies down to a few meV can be reached. Early recombination experiments in this energy range with  $U^{28+}$  produced recombination rates exceeding theoretical predictions for RR by a factor of 200 [2]. Measurements on  $Au^{50+}$  [3] and  $Pb^{53+}$  [4] yielded similar effects. In these ions most of the excess rate stems from unidentified DR resonances close to zero collision energy, and due to the complexity of the atomic structure it is presently not feasible to compare low-energy recombination experiments with theory in a meaningful way in these many-electron systems. However, investigations with bare ions—where

DR cannot occur—also showed a recombination rate enhancement of up to several times the expected RR rate for relative energies below  $\approx 10$  meV [5–9]. Qualitatively, all experiments consistently show that recombination rates for ions almost at rest in a cold, magnetized electron gas can considerably exceed the rates predicted by averaging cross sections for field-free RR over an electron ensemble unperturbed by the presence of external fields and the Coulomb field of the ion; neglecting three-body recombination in such a calculation is justified by the relatively large binding energies of the observable final states  $n_f$ , the low electron density, and the absence of a marked electron density dependence [10–12]. On a quantitative level, results for the enhancement factor obtained at different laboratories or even in different measurements at the same facility have so far been fluctuating in an uncontrolled manner. Thus, the importance of applied external fields and the beam temperatures, varying among previous studies, was unclear. In this paper we report on a detailed study in  $C^{6+}$  and  $F^{6+}$ , where we observe distinct magnetic field and beam temperature dependences explaining the scatter of previous results. Bare carbon is a clean system without uncertainties connected with DR structure. Li-like fluorine, on the other hand, features DR close to  $E = 0$ , and its recombination spectrum has been calculated accurately [13]. This offers useful opportunities of *in situ* temperature diagnostics and can answer whether or not the rate enhancement also occurs in the dielectronic capture of very slow electrons.

So far, all evidence in this matter has been obtained at electron coolers or targets, which use longitudinal magnetic guiding fields between 20 and 590 mT to prevent the electron beam from blowing up due to its own space charge. Theory, on the other hand, considers the recombination in free space. This Letter aims at clarifying the influence of the conditions in the electron cooler. The magnetic field, the electron density, the ion density, and the beam temperatures were for the first time all varied

systematically in a well-controlled manner. As novel effects, we establish the dependence of the excess recombination rate on the magnetic guiding field strength and on the longitudinal energy spread.

The experiment was carried out at the heavy-ion storage ring TSR at the Max-Planck-Institut für Kernphysik in Heidelberg on stored beams of  $F^{6+}$  and  $C^{6+}$  ions at energies of 74 and 47 MeV, respectively (resulting in identical velocities  $\beta = 0.09$ ), with beam currents between 10 and 400  $\mu A$ . The ions are merged in the storage ring with a magnetically guided electron beam; the straight overlap region of 1.5 m is defined by a solenoid and is delimited by magnetic toroidal deflectors with 0.8 m bending radius. The purpose is to electron-cool the ions and to provide electrons for recombination experiments. The details of the measuring procedure are described in [14]. The average motion of the electron beam with respect to the ion beam is characterized by the relative energy  $E$  (which vanishes for matched beam velocities), and the effective collision energies follow from the velocity spreads of the electrons and ions, which for both beams are different in the longitudinal and the transverse direction. Longitudinally, the velocity spread of the electrons is strongly reduced through their acceleration and typically corresponds to a temperature of  $kT_{\parallel e} \approx 0.06$  meV. The longitudinal velocity spread of the ion beam increases with the ion current because of intra-beam scattering and therefore can contribute to the spread of the longitudinal relative velocity between the electrons and the ions. Transversely the electron velocity spread is reduced through adiabatic magnetic expansion by a sufficiently slow transfer of the electrons from a region of high magnetic field strength  $B_c$  surrounding the cathode (at temperature  $T_c$ ) into a region of lower field strength  $B$ , thus reaching electron temperatures of  $T_{\perp e} = T_c/\zeta$ , where  $\zeta = B_c/B$  is the expansion factor. Currently,  $\zeta_{\max} = 26$  is possible at TSR, corresponding to  $kT_{\perp e} \approx 5$  meV. The transverse ion velocity spread yields only a small contribution to the relative electron-ion velocities. The resulting spread of the relative velocities of the electrons with respect to the ions will be expressed by temperatures  $T_{\parallel}$  and  $T_{\perp}$ , with  $T_{\parallel} < T_{\perp}/30$  in all cases. For a direct *in situ* measurement of the spread of relative velocities we analyzed the observed line shape of a narrow DR resonance in  $F^{6+}$  at 10 meV to separately determine  $T_{\parallel}$  and  $T_{\perp}$ . For the  $C^{6+}$  beam, stored with the same velocity and hence with identical electron-cooler settings, the temperatures were inferred from the fluorine measurements.

As mentioned above, the presence of ignored DR resonances around  $E = 0$  can potentially give a false rate enhancement contribution. For Li-like  $F^{6+}$ , however, a precise calculation, based on relativistic many-body perturbation theory, of the  $1s^2 2s(2S) + e^- \rightarrow 1s^2 2p(2P)6l$  resonances in the region  $E < 0.6$  eV reproduces the observed spectrum very well and shows that the DR spectrum is sufficiently well understood for our study [13]. In order to establish the expected “conventional” spectrum,

the calculated rate has to be convoluted with the proper velocity distribution parametrized by  $T_{\perp}$  and  $T_{\parallel}$ . Figure 1(a) shows the recombination energy spectrum for  $F^{6+}$  and the essentials of the temperature fit; the resonance at 10 meV [assigned to  $2p(2P_{3/2})6p^2P_2$ ] is a hyperfine doublet separated by 0.3 meV with calculated intrinsic line widths of 0.1 meV. The asymmetric shape originates from the anisotropic velocity distribution: the steep rise on the right is essentially determined by  $T_{\parallel}$ , the left flank by  $T_{\perp}$ . “Background” such as RR, tails from DR lines at higher energies and a contribution from a broad DR resonance predicted to lie at 7 meV (assignment  $2p(2P_{3/2})6p^2P_1$ , natural width 25 meV) are important enough to require inclusion into the fit. DR and RR as calculated and fitted to the resonances comprise the “expected” rate shown shaded. The remaining unshaded part below the data points is identified as the excess rate  $\Delta\alpha(E)$ , and as a measure for its magnitude in a particular measurement we use its value at  $E = 0$ , denoted as  $\Delta\alpha$ . The fit results are robust against variations of the width and the hyperfine splitting of the 10 meV resonance; also, the exact parameters of the background fit, while slightly influencing the absolute size of  $\Delta\alpha$ , do not significantly influence its dependence on the beam temperature, density, and magnetic field. Recombination energy spectra for  $C^{6+}$ , such as the example of Fig. 1(b), are interpreted by direct comparison to the

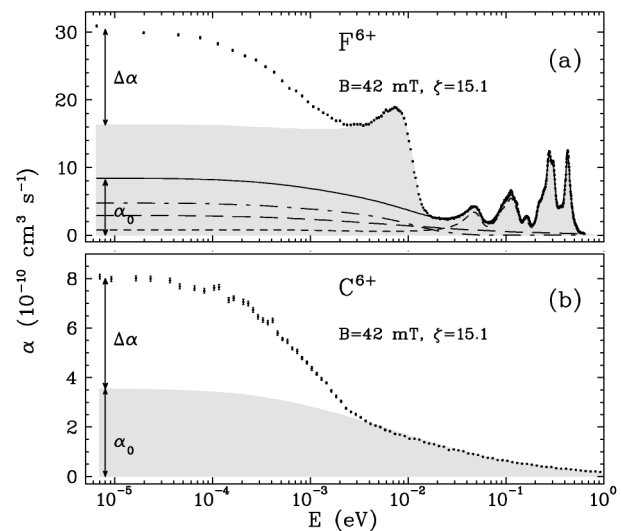


FIG. 1. (a) Recombination spectrum of  $F^{6+}$ . Resonances are due to dielectronic recombination  $[F^{6+}]1s^2 2s(2S) + e^- \rightarrow [F^{5+}]1s^2 2p(2P)6l$ . Shaded area: calculated rate from RR (long-dashed line), a broad DR line at 7 meV (dashed-dotted line), all DR lines above 20 meV (short-dashed line), and from the narrow DR line at 10 meV (above the solid line). The solid line is the sum of the first three contributions. Only these, combined into  $\alpha_0$ , contribute significantly to the cross section below 3 meV. In comparison, the cross section from the narrow resonance at 10 meV is very small below 3 meV, even if the velocity averaging gives the rate a significant tail. The unshaded area below the data points is the excess rate. (b) Recombination in  $C^{6+}$ . The shaded part is RR theory.

calculated RR rate and extraction of the excess  $\Delta\alpha$  at  $E = 0$ . For both  $C^{6+}$  and  $F^{6+}$  the observed excess rates have energy dependences similar to each other and to the earlier observations [6,7,9].

The four-dimensional space of externally controlled parameters—the magnetic field  $B$ , the expansion  $\zeta$ , the electron density  $n_e$ , and the ion current  $I_i$ —was primarily investigated by varying one quantity while leaving the others at “standard” settings typically used in TSR recombination experiments. Analysis of the spectra showed that the variation of  $T_\perp$  through changes in  $\zeta$  results in the cleanest variation of a single parameter, as  $T_\parallel$  remains unaffected. Figure 2(a) shows the dependence of the excess recombination rate  $\Delta\alpha$  on the transverse temperature for  $F^{6+}$  and, from an earlier TSR measurement [15], for  $C^{6+}$ . The scaling of  $\Delta\alpha$  is well represented by  $T_\perp^{-1/2}$  over a wide range of transverse temperatures; since the rates from RR and from DR resonances with significant tails at  $E = 0$  (their sum is denoted  $\alpha_0$  in Fig. 1) also show this scaling, we find  $\Delta\alpha(T_\perp) = \text{const} \times \alpha_0(T_\perp)$ , compatible with the possibility that  $\Delta\alpha$  stems from an “enhancement” of these processes at low energies. Next,  $\Delta\alpha$  is examined as a function of the ion current  $I_i$ . Since its variation causes an accompanying change of  $T_\parallel$ , we extract this parameter from the line shape of the 10 meV DR resonance and interpret the variation of  $\Delta\alpha$  as caused by the change in  $T_\parallel$ . The ion beam current also slightly affects  $T_\perp$ ; however the influence of  $T_\perp$  has been established above, and its impact can be removed by plotting a modified excess recombination rate  $\Delta\alpha\sqrt{kT_\perp}$  as shown in Fig. 2(b). For three different magnetic field settings in  $F^{6+}$  and one in  $C^{6+}$ , we observe a  $T_\parallel^{-1/2}$  scaling of  $\Delta\alpha\sqrt{kT_\perp}$ . This indicates that the enhancement depends on how well the *longitudinal* velocities of the electrons and ions are matched. In contrast, the conventional rate,

obtained from a convolution of an isotropic cross section, depends on the *total* relative velocity, which on average is almost independent of  $T_\parallel$ , since  $T_\parallel \ll T_\perp$ . It is interesting to note that a variation of  $T_\perp$  leaves the shape of the excess “bump” unchanged, and that the energy-integrated excess rate scales as  $T_\perp^{-1/2}$ , while, on the other hand, an increase of  $T_\parallel$  broadens the bump, but the integral excess rate remains constant.

Variations of  $B$  and  $n_e$  inevitably alter the temperatures. The observed influence of  $T_\parallel$  and  $T_\perp$  on  $\Delta\alpha$  suggests that one should look at a scaled excess recombination rate  $\Delta\tilde{\alpha} = \Delta\alpha\sqrt{kT_\perp kT_\parallel}$ . The variation of  $B$  was limited by the minimum field required to guide the electron beam (20 mT) and the maximum magnet current (70 mT). Figure 3(a) displays the response of  $T_\perp$  to the change of the magnetic field in  $F^{6+}$ . At fields below 35 mT,  $T_\perp$  strongly rises. Most likely this stems from the increasing nonadiabaticity of the magnetic beam guiding for low fields, and this demonstrates the necessity to determine  $T_\perp$  experimentally. Above 35 mT,  $T_\perp$  is essentially flat.  $T_\parallel$  shows no significant dependence on the field. In the upper trace of Fig. 3(b) a strong rise of  $\Delta\tilde{\alpha}$  with increasing magnetic field is seen for  $F^{6+}$ . The lower trace of Fig. 3(b) shows the results for carbon, exhibiting the same behavior. Our temperature-corrected rate  $\Delta\tilde{\alpha}$  plotted versus  $n_e$  (Fig. 4) shows no significant electron density effect, in agreement with previous measurements conducted without temperature monitoring [10,11].

Since the excess is present in bare ions, it has been speculated that it originates in an enhancement of RR at low energies. However, it is apparent from Figs. 2(b) and 3 that the excess rate is much higher in  $F^{6+}$  than in  $C^{6+}$ , although the RR rate is roughly equal for both ions. Assuming that the total expected rate with nonzero cross section at  $E \lesssim 3$  meV is subject to enhancement in  $F^{6+}$ , the

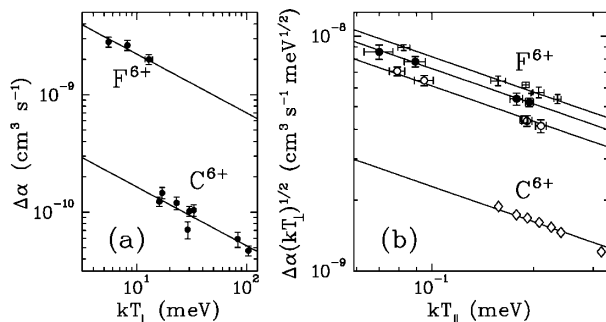


FIG. 2. Excess recombination rate as a function of temperature. (a) Transverse temperature:  $F^{6+}$  data taken at  $B = 42$  mT for  $\zeta = 25.6, 15.1,$  and  $9.6$ .  $C^{6+}$  data taken from [15] (the errors correspond to an estimated 3% relative uncertainty of the rate measurement). Solid lines are fits to  $T_\perp^{-1/2}$ . (b) Longitudinal temperature:  $F^{6+}$  data for three magnetic fields,  $B_0 = 35$  mT ( $\circ$ ),  $42$  mT ( $\bullet$ ), and  $60$  mT ( $+$ );  $\zeta = 15.1$ .  $C^{6+}$  data ( $\diamond$ ) at  $42$  mT and  $\zeta = 15.1$ . The lines are fits to  $T_\parallel^{-1/2}$ .  $T_\parallel$  for  $C^{6+}$  is inferred from  $F^{6+}$  data.

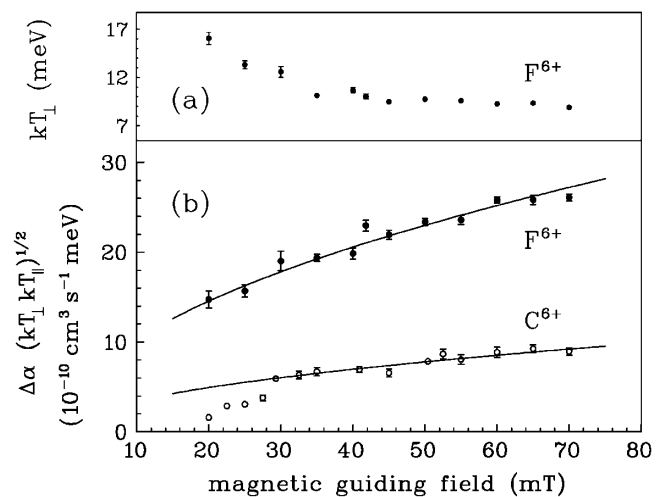


FIG. 3. Magnetic field dependence of the excess recombination rate (b) in  $F^{6+}$  and  $C^{6+}$ , and of  $T_\perp$  (a). Lines  $\propto \sqrt{B}$  are drawn to guide the eye;  $\zeta = 15.1, n_e \approx 7 \times 10^6 \text{ cm}^{-3}$ .

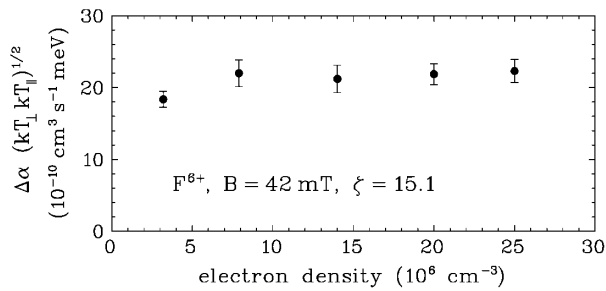


FIG. 4. Excess recombination rate in  $F^{6+}$  as a function of the electron density in the interaction zone.

relative enhancement at  $E = 0$ , given by  $\Delta\alpha/\alpha_0$  (see Fig. 1), is roughly comparable in both ions: as a specific example, at  $B = 70$  mT and  $kT_{\parallel} = 0.2$  meV,  $\Delta\alpha/\alpha_0$  amounts to 2.0 and 1.85 for  $F^{6+}$  and  $C^{6+}$ , respectively. This indicates that the enhancement mechanism might be independent of the specific recombination process.

The observed sensitivity of the enhancement to both the magnetic field and the longitudinal relative velocity spread could be a key to an explanation of the effect. It has been estimated that the influence of a magnetic field on the RR cross section in a single electron-ion collision should be negligible for our field strengths [16]. Field enhancement of the DR cross section [17,18] is known to be caused by level mixing of high-Rydberg capture resonances; in our case of a capture into  $n = 6$  this effect is also unsubstantial. However, the magnetic field strongly influences the electron dynamics on a length scale of the order of the electron-cyclotron radius ( $\approx 5 \mu\text{m}$  for  $kT_{\perp} = 5$  meV and  $B = 40$  mT) and makes it dependent mainly on the longitudinal relative velocities (the transverse degrees of freedom being cyclic). For a steady-state situation in the interaction region, plasma screening of the ions in the magnetized co-moving electron gas may lead to a significant increase of the local electron density [19]. Magnetized electron beams found in electron coolers were shown to have plasma parameters  $\Gamma$  of order 1, essentially independent of their density; the related constant *relative* increase of the local electron density could explain the absence of a density dependence for  $\Delta\alpha$ . Alternatively, transient fields seen by an ion entering the electron beam through the toroidal inflector typically vary on a nanosecond time scale and could transfer slow electrons onto long-range bound orbits, the dynamics being governed by the magnetic guiding field. The average effect of such processes could again be described by an increase of the local electron density near the ions. Enhanced recombination may hence be re-

garded as a sensitive probe for such density increases at very low relative velocity.

In conclusion, the detailed study of the low-energy excess recombination rate as a function of external parameters in connection with beam temperature diagnostics allowed us to clearly identify distinct dependences for the first time. A comparison of the excess rates in  $F^{6+}$  and  $C^{6+}$  suggests that they are independent of the specific recombination mechanism. This finding and the observed dependences on  $B$  and  $T_{\parallel}$  point to a possible explanation of the recombination enhancement by an increased density of slow electrons near the ion, developing during the passage through the electron target in the combined Coulomb and external magnetic fields.

We acknowledge support from the German Federal Minister of Education and Research (BMBF), through contracts No. 06 GI 848 and No. 06 HD 854, and from the Swedish Natural Science Research Council (NFR).

---

\*Present address: Mid-Sweden University, Sundsvall, Sweden.

- [1] S. Schippers, Phys. Scr. **T80**, 158 (1999).
- [2] A. Müller *et al.*, Phys. Scr. **T37**, 62 (1991).
- [3] O. Uwira *et al.*, Hyperfine Interact. **108**, 149 (1997).
- [4] S. Baird *et al.*, Phys. Lett. B **361**, 184 (1995).
- [5] A. Wolf *et al.*, in *Atomic Physics 13*, edited by T.W. Hänsch, H. Walther, and B. Neizert, AIP Conf. Proc. No. 275 (AIP, New York, 1993), p. 228.
- [6] H. Gao *et al.*, Phys. Rev. Lett. **75**, 4381 (1995).
- [7] O. Uwira *et al.*, Hyperfine Interact. **108**, 167 (1997).
- [8] U. Schramm *et al.*, Hyperfine Interact. **108**, 273 (1997).
- [9] H. Gao *et al.*, J. Phys. B **30**, L499 (1997).
- [10] H. Gao *et al.*, Hyperfine Interact. **99**, 301 (1996).
- [11] A. Hoffknecht *et al.*, J. Phys. B **31**, 2415 (1998).
- [12] M. Pajek and R. Schuch, Hyperfine Interact. **108**, 185 (1997).
- [13] E. Lindroth and M. Tokman, *Proceedings of the XXI ICPEAC, Sendai, Japan, 1999, Abstracts of Contributed Papers*, edited by Y. Itikawa *et al.* (University of Electro-Communications, Tokyo, 1999), p. 388; W. Zong *et al.*, Phys. Rev. A **56**, 386 (1997).
- [14] G. Kilgus *et al.*, Phys. Rev. A **46**, 5730 (1992).
- [15] U. Schramm *et al.*, Hyperfine Interact. **99**, 309 (1996).
- [16] V.M. Katkov and V.M. Strakhovenko, Sov. Phys. JETP **48**, 639 (1978).
- [17] F. Robicheaux *et al.*, Phys. Rev. Lett. **80**, 1402 (1998); W. A. Huber and C. Bottcher, J. Phys. B **13**, L399 (1980).
- [18] T. Bartsch *et al.*, Phys. Rev. Lett. **82**, 3779 (1999).
- [19] Q. Spreiter *et al.*, Hyperfine Interact. **114**, 245 (1998).